

## A NEW TYPE OF SPIN ORDERING IN THE SYSTEM OF HEXAGONAL

 $Ba_{2-x}Sr_xZn_2Fe_{12}O_{22}(Y)$  FERRITES

V. A. SIZOV, R. A. SIZOV, and I. I. YAMZIN

Institute of Crystallography, Academy of Sciences, U.S.S.R.

Submitted July 10, 1967

Zh. Eksp. Teor. Fiz. 53, 1256–1267 (October, 1967)

A neutron diffraction investigation of the system of hexagonal  $Ba_{2-x}Sr_xZn_2Fe_{12}O_{22}(Y)$  ferrites was carried out in the temperature range from 4.2°K up to the Curie point (400°K) and in magnetic fields up to 20,000 Oe. The existence of a magnetic superstructure in the neutron diffraction patterns is explained on the basis of a quasi-helical magnetic structure model which combines collinearity of the spins in crystallographically different blocks of the unit cell and helical ordering of the spin axes of the blocks relative to each other. A brief analysis of the causes leading to the appearance of quasi-helical ordering is presented.

## 1. INTRODUCTION

THE purpose of this work was to investigate spin ordering in hexagonal ferrites of the  $Ba_{2-x}Sr_xZn_2Fe_{12}O_{22}$  system (type-Y structure).

The hexagonal ferrites are multicomponent magnetic oxides with a complex crystal structure possessing a large magnetic anisotropy; they came to be objects of investigation considerably later than those with a cubic crystal structure. In the meantime work proceeded on the synthesis of new hexagonal ferrites and more than thirty types of structures, differing in symmetry, the size of their unit cells, and the number of atoms these contain (from several dozens to several hundred atoms per unit cell), are known at present. The atomic structure of these compounds was investigated by a number of authors.<sup>[1-3]</sup> They established the close relationship between the different hexagonal ferrites which represent polytype structures formed of uniform structural elements. For hexagonal ferrites with the smallest number of atoms in the unit cell Braun<sup>[1]</sup> established five basic structure types which were denoted by the symbols M, W, X, Y, and Z.

Standard structural elements of which all hexagonal ferrites are formed are four or six-layer units or blocks of close-packed oxygen ions perpendicular to the C axis of the crystal. These blocks are occupied by  $Me^{2+}$  and  $Me^{3+}$  cations (di- or trivalent iron, other elements of the iron group, zinc, magnesium etc.), in analogy with the spinel ferrites. These "spinel" blocks are connected to each other by connecting blocks consisting of one or two oxygen layers in which, each of four oxygens is replaced by a large divalent cation (barium, lead, strontium, etc.). The structures of all hexagonal ferrites consist of spinel blocks and of connecting blocks following each other in various combinations and sequences.

The chemical formula of a type-Y hexagonal ferrite can in its general form be written:  $A_2Me_2^{2+}Me_{12}^{3+}O_{22}$  where A is a large divalent cation, for example  $Ba^{2+}$ ;  $Me^{2+}$  is a divalent cation of smaller size, usually  $Zn^{2+}$ , but it can be  $Co^{2+}$ ,  $Fe^{2+}$  etc.;  $Me^{3+}$  is usually  $Fe^{3+}$ . There are three formula units per unit cell. The crystal

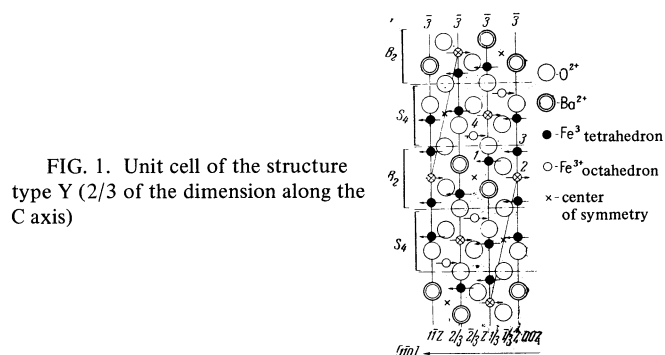


FIG. 1. Unit cell of the structure type Y (2/3 of the dimension along the C axis)

structure can be represented schematically in the form  $S_4-B_2-S_4-B_2 \dots$ . Here  $S_4$  are four-layer spinel blocks and  $B_2$  two-layer connecting blocks which alternate along the C axis. Type-Y ferrites have the space group  $R\bar{3}m$ .

Figure 1 shows the atomic structure of the simplest hexagonal type-Y ferrite:  $Ba_2Zn_2Fe_{12}O_{22}$ .<sup>[1]</sup> The projection of the structure on the (110) is presented. The figure encompasses two thirds of the unit cell along the C axis. The unit cell parameters are:  $a = 5.87 \text{ \AA}$  and  $c = 43.56 \text{ \AA}$ . The a parameter remains practically unchanged for all the possible variations of the chemical composition; the c parameter is more sensitive to these variations and can change by several hundredths or tenths of an Ångström. The positions of the atoms in the unit cell are:<sup>[1]</sup>

Fe	3a	$x = 0$	$z = 0$	O	18h	$x = -0.17$	$z = 0.085$
O	18h	0.15	0.027	Fe	18h	0.503	0.110
Ba	6c	$2/3$	0.0336	O	6c	$2/3$	0.136
$1/2 (Fe + Zn)$	6c	$1/3$	0.0428	O	18h	0.17	0.138
Fe	6c	0	0.0656	$1/2 (Fe + Zn)$	6c	0	0.152
O	6c	$1/3$	0.084	Fe	3b	$1/3$	$1/6$

As regards the determination of the magnetic structure of the hexagonal ferrites, i.e., the determination of the position of the magnetic ions in the crystal lattice and of the orientation of their spins, the first attempt in this direction was made by Gorter<sup>[4]</sup> who used the assumptions of the indirect exchange theory of Anderson<sup>[5]</sup> and Kramers<sup>[6]</sup> for an approximate estimate of the ratio of the exchange energy for various pairs of ions,

and proposed models of magnetic structures for each one of the basic structure types: M, W, X, Y, and Z. In doing this, he assumed that the crystal structure of the ferrites contains no other cations except  $\text{Ba}^{2+}$ ,  $\text{Zn}^{2+}$ ,  $\text{Fe}^{2+}$  and  $\text{Fe}^{3+}$ .

In the Gorter models the spins are collinear, along the hexagonal C axis (structures M, X, and Z), or in the basal plane (Y structure). These models are in satisfactory agreement with the magnetic properties of hexagonal ferrites, and there was no doubt that they are correct. In two instances they were confirmed by the results of neutron diffraction studies carried out on the ferrite  $\text{BaFe}_{12}\text{O}_{19}$  (type M),<sup>[7]</sup> and on the Y-type ferrite  $\text{Ba}_2\text{Zn}_2\text{Fe}_{12}\text{O}_{22}$ .<sup>[8]</sup> In Fig. 1 arrows indicate the spin orientation corresponding to the Gorter model.

However, along with the hexagonal ferrites that contain no other magnetic ions, except for iron ions, a large number of compounds is known which belong to the basic structure types M, W, X, Z, and Y in which the  $\text{Fe}^{2+}$  and  $\text{Fe}^{3+}$  ions are partly or completely replaced by ions of cobalt, manganese, titanium, and other elements.<sup>[9]</sup> In certain cases there are also considerable differences in the magnetic properties of the substituted and unsubstituted ferrites. In particular, in cobalt-substituted ferrites of the type W Bickford<sup>[10]</sup> and Perekalina and Zalesskii<sup>[11]</sup> observed a complicated picture of the magnetic crystallographic anisotropy. The neutron diffraction investigation of the magnetic structure of these ferrites which we carried out<sup>[12]</sup> showed that although the magnetic structure remains collinear, the spin axes deviate from an orientation parallel to the C axis, making an angle with the C axis which depends on the cobalt content and on the temperature.

In investigations of the magnetic properties of the ferrite  $\text{Ba}_{2-x}\text{Sr}_x\text{Zn}_2\text{Fe}_{12}\text{O}_{22}$  (Y) Enz<sup>[13]</sup> observed the anomalous nature of the torque and magnetization curves. The Gorter model of the magnetic structure could not explain the observed effects and Enz assumed in this instance the existence of a helicoidal spin ordering. This assumption was based on the idea that in substituting the barium ions by strontium the large difference between the ionic radii ( $\text{Ba} - 1.43 \text{ \AA}$ ,  $\text{Sr} - 1.27 \text{ \AA}$ ) should result in a local distortion of the crystal structure with a shift of the  $\text{Fe}^{3+}$  ions which lie close to the Ba (Sr) ions. In such a shift one can expect a change in the values of the exchange interaction between certain pairs of magnetic ions and a corresponding change in the type of the magnetic structure, in particular a disturbance of the collinearity in the latter. Enz's hypothesis remained unconfirmed, since the spin configuration was not established by neutron diffraction. The only neutron-diffraction investigation of a Y-type ferrite<sup>[8]</sup> was carried out on the  $\text{Ba}_2\text{Zn}_2\text{Fe}_{12}\text{O}_{22}$  ferrite for which no deviations from the plane Gorter model were found.

## 2. EXPERIMENTAL PART

A. The samples were single crystals of ferrites of the  $\text{Ba}_{2-x}\text{Sr}_x\text{Zn}_2\text{Fe}_{12}\text{O}_{22}$  system with a strontium content  $x$  per formula unit of 0, 1.0, 1.2, 1.4, and 1.6. The crystals were grown by the method of spontaneous crystallization from a solution in the melt with slow cooling of the latter. Just as Enz,<sup>[13]</sup> we were unable

to achieve complete substitution of barium by strontium. For strontium contents larger than  $x = 1.6$  the crystallization product consisted in the main of crystals of other phases: spinel, M, W, and Z. Crystals of the Y phase were mostly in the form of hexagonal platelets of various dimensions. In some cases these attained cross sections of 7–8 mm and a thickness of 0.8–2.5 mm.

Diffraction patterns of the basal plane of the crystals were obtained on an URS-501 (Fe  $K\alpha$  radiation) x-ray unit. For further investigation we chose crystals whose diffraction patterns contained only lines corresponding to the Y phase. For these crystals we determined the values of the  $c$  parameter of the unit cell making use of reflections at  $2\theta$  angles larger than  $100^\circ$ . The strontium content in the crystals was measured by the x-ray fluorescence method. The discrepancy between the measured values and the mixture content of strontium did not exceed  $\pm 5$  percent. The obtained results are presented in Table I.

B. The neutron diffraction measurements were carried out on single-crystal samples in the form of a prism with a rectangular cross section of  $1 \times 2$  mm and a height of 3–5 mm. We measured the intensity of the diffraction peaks [mainly of the (00 $l$ ) planes] and its dependence on the temperature, direction and intensity of the external magnetic field imposed on the sample. We investigated the range of temperatures of 4.2–400° K and of fields 0–20,000 Oe directed parallel and perpendicular to the scattering vector  $\epsilon$ .

In the 77–293° K temperature range the investigations were carried out in a cryostat equipped with a device for heating the sample. The temperature at which the sample was being investigated was determined with the aid of a thermocouple. The error in these measurements did not exceed 5°.

The measurements were carried out on neutron diffractometers<sup>[14,15]</sup> with  $\lambda = 1.07 \text{ \AA}$ . The intensity was measured in steps of 10 minutes of angle with simultaneous  $\theta : 2\theta$  displacement of the sample and of the neutron detector. The integrated intensity was obtained by weighing the areas enclosed between the outlines of the diffraction peaks and the background line.

C. The neutron diffraction patterns are characterized by the presence of structure reflections corresponding to the space group  $R\bar{3}m$  and to the unit cell parameters presented in Table I. These structure reflections contain along with nuclear contributions also more or less appreciable magnetic contributions.

With the replacement of barium by strontium the diffraction pattern changes considerably, this being particularly noticeable for  $x > 1$ . Broadening of reflections containing considerable magnetic contributions is observed; for large strontium contents this is followed by a splitting off of superstructure magnetic reflections (satellites) from the structure reflections. It is seen from Fig. 2 which depicts the angular region near the 009 reflection (which contains the largest magnetic contribution) that as the strontium content increases there is an increase in the distance of the satellites from the structure reflection which is also accompanied by considerable change in their intensity.

D. It turned out that the superstructure reflections observed in the diffraction pattern could not be indexed on the basis of the unit cell of the investigated ferrites,

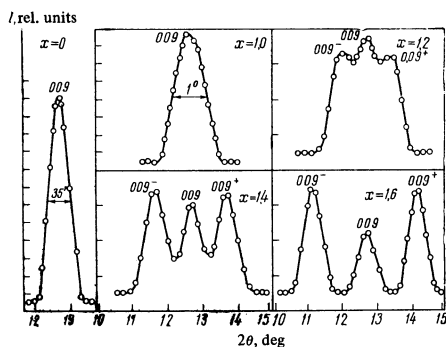


FIG. 2. Diffraction peaks in the region of the 009 reflection as a function of the composition of the investigated samples at a temperature of 293°K.

even by increasing them within reasonable limits. We have denoted them by  $00l^\pm$ , as is usual for satellites appearing in the case of helical spin ordering, because the observed splitting of the magnetic reflections is characteristic for the diffraction of neutrons by helical magnetic structures.

Assuming the existence of the superstructure to be due to helical spin ordering, one can determine from the positions of the satellites in the diffraction pattern its repeat distance  $\tau$  from the expression

$$\frac{1}{\tau} = \frac{1}{d_{hkl}} \pm \frac{1}{d_{hkl}^\pm},$$

where  $d_{hkl}$  and  $d_{hkl}^\pm$  are the interplanar distances for  $hkl$  and  $hkl^\pm$  reflections.

Measurements of the repeat distances  $\tau$  of the magnetic superstructure for various compositions as a function of temperature and external magnetic field showed that within the error of the measurements the values of  $\tau$  are multiples of  $1/3$  of the unit-cell dimension along the C axis. Repeat distances  $\tau$  were observed which were close to  $2/3c$ ,  $4/3c$ ,  $5/3c$ , and  $2c$ .

E. The temperature dependence of the repeat distance of the superstructure for various compositions is given in Table II. With increasing strontium content (with the temperature constant) the repeat distance  $\tau$  decreases. At the same time, for all compositions the repeat distance remains constant within broad temperature ranges, except for narrow temperature intervals characteristic for each composition; these occur in the 220–270 and 310–355°K ranges where  $\tau$  changes abruptly.

F. Switching on a magnetic field perpendicular to the scattering vector  $\epsilon$ , i.e., in the basal plane of the crystal also causes a change in the positions of the satellites and in their intensities. Figure 3 shows diffrac-

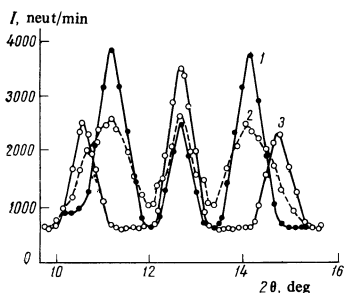


FIG. 3. Neutron diffraction patterns of a  $\text{Ba}_{0.4}\text{Sr}_{1.6}\text{Zn}_2\text{Fe}_{12}\text{O}_{22}$  in magnetic fields  $\mathbf{H} \perp \epsilon$ : 1 –  $H = 0$ , 2 –  $H = 800$  Oe, 3 –  $H = 1500$  Oe.

Table I. Dependence of the c parameter of the unit cell of ferrites of the  $(\text{Ba}, \text{Sr})_2\text{Zn}_2\text{Fe}_{12}\text{O}_{22}$  system on the chemical composition

Composition	$c$ , Å ( $\pm 0.005$ Å)
$\text{Ba}_2\text{Zn}_2\text{Fe}_{12}\text{O}_{22}$	43.565
$\text{Ba}_{1.0}\text{Sr}_{1.0}\text{Zn}_2\text{Fe}_{12}\text{O}_{22}$	43.517
$\text{Ba}_{0.8}\text{Sr}_{1.2}\text{Zn}_2\text{Fe}_{12}\text{O}_{22}$	43.490
$\text{Ba}_{0.6}\text{Sr}_{1.4}\text{Zn}_2\text{Fe}_{12}\text{O}_{22}$	43.488
$\text{Ba}_{0.4}\text{Sr}_{1.6}\text{Zn}_2\text{Fe}_{12}\text{O}_{22}$	43.477

tion patterns obtained at 20°C with crystals of composition  $x = 1.6$  (the vicinity of the 009 reflection) in fields perpendicular to  $\epsilon$  and of magnitude 0, 800, and 1500 Oe. From the spacing between the satellites it follows that in weak fields  $H = 800$  Oe the repeat distance of the magnetic superstructure is practically constant,  $\tau_1 = 43$  Å. With increasing fields the repeat distance decreases rapidly to a value  $\tau_2 = 29$  Å, and then remains constant until the helical ordering is entirely destroyed (the satellites disappear) in fields larger than 8000 Oe.

Table II. Temperature dependence of the magnetic superstructure repeat distance

Chemical composition	$\tau$ , Å			
	4–29°K	77°K	293°K	360°K
$\text{Ba}_{0.8}\text{Sr}_{1.2}\text{Zn}_2\text{Fe}_{12}\text{O}_{22}$	85.6	86.0	76.2	63.2
$\text{Ba}_{0.6}\text{Sr}_{1.4}\text{Zn}_2\text{Fe}_{12}\text{O}_{22}$	74.8	74.0	61.3	43.9
$\text{Ba}_{0.4}\text{Sr}_{1.6}\text{Zn}_2\text{Fe}_{12}\text{O}_{22}$	60.0	59.0	43.8	31.6

A strong broadening of the satellites and a distortion of their shape is observed in the diffraction pattern in the temperature and field ranges in which a jumpwise change of  $\tau$  occurs; this can apparently be explained by the existence of regions with superstructure repeat distances  $\tau_1$  and  $\tau_2$  in the crystal.

Switching on a magnetic field parallel to the scattering vector  $\epsilon$ , i.e., along the C axis of the crystal, leads to a gradual decrease in the intensity of the superstructure reflections with increasing field intensity until their complete disappearance in fields above 16,000 Oe.

The change in the position of the satellites and in their intensity is accompanied in the indicated transition regions of magnetic fields by a sharp change in the intensities of the magnetic structure reflections. Thus, on switching a magnetic field  $\mathbf{H} \perp \epsilon$  the intensity of the 009 structure reflection undergoes two jumplike changes: at  $H = 800$ –1000 Oe and for  $H = 7000$ –8000 Oe, i.e., when the repeat distance of the magnetic superstructure changes from 43 to 29 Å (first jump), and when the magnetic superstructure disappears (second jump) (see Fig. 4). The change in the intensity of

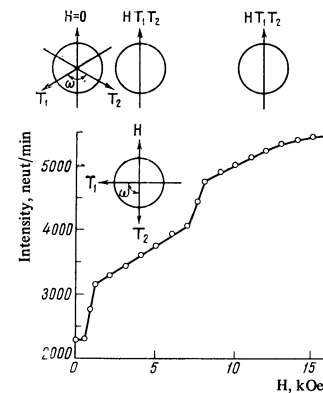


FIG. 4. Dependence of the intensity of the structure reflection 009 (composition  $x = 1.6$ ) on the intensity of the magnetic field  $\mathbf{H} \perp \epsilon$  at 293°K.

the structure reflection between both of these jumps and in fields above 8000 Oe can be related to the domain mechanism of magnetization in the basal plane.

In the absence of a field at a temperature above 370–380°K, i.e., after the disintegration of the magnetic superstructure, one notes the appearance of a magnetic contribution to  $h0l$  structure reflections, a fact which attests to the reorientation of spins from directions perpendicular to the C axis to a direction parallel to it. This is also confirmed by the results of magnetic measurements carried out in [16]. At 400°K (the Curie point) all magnetic reflections disappear.

### 3. POSSIBLE MODELS OF THE MAGNETIC STRUCTURE

We have considered two models of the magnetic structure that explain best the observed neutron diffraction pattern.

The first is a helical structure of the usual kind with spins lying in the basal plane. Helical magnetic structures have been investigated in a series of theoretical and experimental works. [17–23] Starting from the peculiarities of the exchange interactions in the lattice of a hexagonal type-Y ferrite, one can estimate the phase angles of the cation spins in the various sublattices which participate in the helical ordering. As is seen from Table III which contains the basic initial data for the calculation of the intensities of the magnetic superstructure reflections on the basis of the helical model, the Fe<sup>3+</sup> cations are distributed over ten sublattices. The angle of rotation of the spins is determined by the wave vector of the helical structure  $|\mathbf{k}| = 2\pi/\tau$ . This structure is helicoidal with the helicoid direction of propagation along the C axis.

The second model which we have called quasihelical differs from the usual helical models in that it combines collinearity with helical ordering. We have considered two variants of this model: I—with a statistical distribution of the zinc ions over the 6c locations ( $z = 0.0428$  and  $z = 0.152$ ), and II—with localization of zinc ions in the 6c locations ( $z = 0.152$ ).

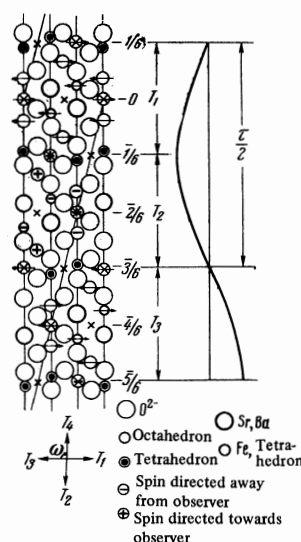
In case I the structure is considered to consist of inequivalent structure blocks S<sub>4</sub> and B<sub>2</sub>. Within these blocks the spins are collinear and parallel to the basal plane. However, the spin axes of the blocks S<sub>4</sub> and B<sub>2</sub> are at an angle to each other. In order to explain the observed neutron diffraction pattern, one must assume the existence of a helical arrangement of the spin axes of the blocks.

In case II it is natural to divide the unit cell along the C axis into three structurally equivalent blocks T, each of which contains six layers of oxygen ions. The boundary between the layers passes through the loca-

Table III. Phase relations between the spin magnetic moments of the Fe<sup>3+</sup> ions in various sublattices

Location of Fe <sup>3+</sup> ion	Phase angle $\alpha$	z parameter	No. of ions in the sublattice	Location of Fe <sup>3+</sup> ion	Phase angle $\Phi$	z parameter	No. of ions in the sublattice
3a	0	0	3	18h	{ 0	0,140	9
6c	{ $\pi$	0,0428	1,5	6c	{ 0	0,223	9
		0,290	1,5			6c	{ $\pi$
6c	{ $\pi$	0,0656	3	3b	{ $\pi$		
		0,269	3			3b	{ 0

FIG. 5. Model of the quasihelical spin structure II with an angle  $\omega = 90^\circ$  at a temperature of 77°K and with a composition of  $x = 1.6$ . On the left is the model of the magnetic structure, on the right is a schematic diagram of the periodicity of the helical wave along the C axis.



tions occupied by the zinc ions. Within the blocks T the spins are collinear and parallel to the basal plane. However, the spin axes of the blocks form an angle  $\omega$  with each other. The spin axes are ordered along a helix with its propagation vector parallel to the C axis. As in the preceding case, the magnitude of the angle  $\omega$ , as well as the repeat distance of the quasihelix, depend on the temperature and on the externally imposed magnetic fields.

The angle  $\omega$  can be obtained from the experimental values of the repeat distance of the superstructure:  $\omega = 2\pi c/3\tau$ . The observed repeat distances  $\tau = 29, 43, 59 \text{ \AA} \dots$  correspond to angles  $\omega = 180, 120, 90^\circ \dots$  (model II).

Figure 5 shows the model of the quasihelical magnetic structure II with an angle  $\omega = 90^\circ$ .

The intensity of the magnetic superstructure reflections due to the helicoidal ordering of spins is given by the expression

$$I_{hkl}^\pm = \frac{1}{2} K \frac{1 + \cos^2 \delta}{2} (F_{\text{mag } hkl}^\pm)^2,$$

where K is a constant which includes geometrical, temperature, absorption factors, etc.,  $\delta$  is the angle between the normal to the plane of rotation of the spins and the scattering vector, and the factor  $1/2$  takes into account the splitting of the magnetic contribution into two satellite reflections.

For the helical model the structure factor of the satellites is of the form

$$F_{hkl}^\pm = \sum_v p_v e^{i\Phi_v} \exp\{2\pi i \mathbf{R}_H^* \cdot \mathbf{r}_v\},$$

where  $p = 0.269 f\mu$ , and  $\Phi_v$  is the phase angle between the spins of the ions in various sublattices

$$\mathbf{R}_H^* = \mathbf{B}_H^* \pm \mathbf{r}^*, \quad \mathbf{B}_H^* = 2\pi \left( \frac{hx}{a} + \frac{ky}{b} + \frac{lz}{c} \right).$$

For the satellite reflections  $00l^\pm$  the structure factor takes on the form

$$F_{00l}^\pm = \sum_v p_v \cos \Phi_v \cos 2\pi(lz_v \pm cz_v/\tau).$$

Analogous expressions can be derived for the quasihelical structure.

For the quasihelical structure I we have

$$F_{hkl}^{\pm} = \sum_m p_m e^{i\Phi_m} \exp\{2\pi\mathbf{B}_H \cdot \mathbf{r}_m\} + \sum_t p_t \exp\{i\Phi_t + i\omega\} \exp\{2\pi\mathbf{B}_H \cdot \mathbf{r}_t\},$$

$$F_{00l}^{\pm} = \sum_m p_m \cos \Phi_m \cos 2\pi l z_m + \sum_t p_t \cos \Phi_t \cos \omega \cos 2\pi l z_t.$$

Here the index  $m$  refers to ions situated in block  $B_2$ , while  $t$  refers to those situated in the block  $S_4$ .

For the quasihelical model II the structure factor is written as for collinear structures:

$$F_{hkl}^{\pm} = \sum_v p_v e^{i\Phi_v} \exp\{2\pi i \mathbf{B}_H \cdot \mathbf{r}_v\},$$

however in the intensity expression for the superstructure reflections the splitting is taken into account by means of the factor

$$q^2 = \frac{1}{2} \left( \frac{1 + \cos^2 \delta}{2} \right)$$

In Table IV we present the intensities of the superstructure reflections, measured and calculated on the basis of three magnetic structure models—the helicoidal and the quasihelical models I and II. In the calculations we made use of the value of the magnetic form factor for  $\text{Fe}^{3+}$  taken from the work of Nathans, Pickart, and Alperin.<sup>[24]</sup> The correction for the thermal vibrations of the atoms at 293 and 355°K was made using the factor  $B = 0.656 \text{ \AA}^2$  adopted from<sup>[1]</sup>. The calculation of the primary and secondary extinction coefficients  $E_p$  and  $E_s$  was carried in accordance with Hamilton's paper.<sup>[25]</sup> The thickness of the mosaic block was taken to be  $t = 10^{-3}$  cm, as determined for the ferrite  $\text{Ba}_2\text{Zn}_2\text{Fe}_{12}\text{O}_{22}$ .<sup>[8]</sup> The angular misorientation parameter of the mosaic blocks  $\eta$  was determined by the use of the nuclear intensities of sixteen 00 $l$  reflections. For the composition  $x = 1.6$  it was 65'' at 77°K and 30'' at 293 and 335°K. The same values of  $\eta$  were employed in taking into account the effect of secondary extinction for other compositions. The correction for the temperature change of the magnetic moment was taken from the curves of the temperature dependence of the magnetization obtained for the investigated ferrites by T. M. Perekalina and kindly placed by her at our disposal.

Table IV shows that for the composition  $x = 1.6$  model II of the quasihelical structure yields the best agreement of the measured and calculated intensities. Satisfactory agreement of the intensities measured and calculated on the basis of model II is also obtained for the composition  $x = 1.4$ . For lower strontium concentrations the accuracy of the intensity measurements of the satellites is low because of the bad resolution. However the complete similarity of the diffraction patterns of ferrites with  $x = 1.0$  to  $x = 1.6$  and the fact that the repeat distances of the superstructure are multiples of one third of the repeat distance  $c$  allows one to conclude that all the investigated compositions have the quasihelical structure II.

The assumption of a quasihelical model of the magnetic structure allows one to explain satisfactorily the changes in the neutron diffraction patterns taking place with changing temperature and the switching on of an external magnetic field illustrated in Table II and Fig. 3.

In the low-temperature region the crystal has a quasihelical magnetic structure with an angle  $\omega = 90^\circ$  between the spin axes of neighboring T blocks ( $\tau = \frac{1}{3}c$ ). At 293°K this angle increases to  $120^\circ$

Table IV. Calculated and measured neutron diffraction intensities from a single crystal of  $\text{Sr}_{1.6}\text{Ba}_{0.4}\text{Zn}_2(\text{Y})$  ferrite

hkl	Calculated intensities of magnetic superstructure reflections $IE_p E_s$			Measured intensity of reflections
	helicical spin configuration	quasihelical model I	quasihelical model II	
$T = 77^\circ \text{ K}$				
003 <sup>-</sup>	169.0	240.0	316.5	280.0
003 <sup>+</sup>	154.0	232.6	244.0	263.2
006 <sup>-</sup>	110.0	7.7	3.0	8.0
006 <sup>+</sup>	98.0	5.6	2.5	6.6
009 <sup>-</sup>	307.0	340.0	648.6	715.0
009 <sup>+</sup>	297.6	339.0	576.7	680.5
0012 <sup>-</sup>	34.4	0.2	14.6	16.0
0012 <sup>+</sup>	27.2	0.1	12.4	14.2
0015 <sup>-</sup>	80.0	97.0	140.0	72.0
0015 <sup>+</sup>	64.4	78.0	128.6	110.0
0018 <sup>-</sup>	144.4	146.2	208.0	231.5
0018 <sup>+</sup>	126.8	127.6	194.0	128.0
0021 <sup>-</sup>	1.4	4.0	31.0	40.0
0021 <sup>+</sup>	1.3	3.3	28.6	36.5
0024 <sup>-</sup>	0.3	0.1	18.4	12.3
0024 <sup>+</sup>	0.2	0	15.2	10.0
$T = 293^\circ \text{ K}$				
003 <sup>-</sup>	4.0	60.0	113.0	102.5
003 <sup>+</sup>	2.9	57.0	88.4	91.0
006 <sup>-</sup>	23.0	12.7	4.6	0
006 <sup>+</sup>	17.0	9.3	4.2	0
009 <sup>-</sup>	63.0	103.4	241.6	298.6
009 <sup>+</sup>	57.0	100.0	212.0	253.5
0012 <sup>-</sup>	13.0	1.0	5.0	13.5
0012 <sup>+</sup>	9.8	0.8	4.5	11.2
0015 <sup>-</sup>	10.0	15.0	42.0	49.8
0015 <sup>+</sup>	8.1	12.2	36.4	19.6
0018 <sup>-</sup>	28.7	22.0	68.0	81.3
0018 <sup>+</sup>	25.2	19.0	60.4	34.8
0021 <sup>-</sup>	0.4	0	8.4	15.7
0021 <sup>+</sup>	0.3	0	6.8	11.4
0024 <sup>-</sup>	0	0.4	4.6	0
0024 <sup>+</sup>	0	0.3	4.0	0
$T = 360^\circ \text{ K}$				
003 <sup>-</sup>	14.0	2.1	46.0	42.5
003 <sup>+</sup>	11.7	1.6	40.0	37.7
006 <sup>-</sup>	6.0	38.6	0	0
006 <sup>+</sup>	4.0	28.2	0	0
009 <sup>-</sup>	29.5	39.6	120.6	103.5
009 <sup>+</sup>	24.5	34.7	98.0	91.6
0012 <sup>-</sup>	5.0	5.8	1.7	0
0012 <sup>+</sup>	3.6	4.5	1.5	0
0015 <sup>-</sup>	1.0	0.2	20.0	9.6
0015 <sup>+</sup>	0.7	0.1	17.6	13.1
0018 <sup>-</sup>	4.3	0	35.3	29.0
0018 <sup>+</sup>	3.3	0	31.5	12.4
0021 <sup>-</sup>	0.3	0	0	0
0021 <sup>+</sup>	0.2	0	0	0
0024 <sup>-</sup>	0	2.0	0	0
0024 <sup>+</sup>	0	1.7	0	0

( $\tau = c$ ), and at 350°K to  $180^\circ$  ( $\tau = \frac{2}{3}c$ ).

The change in the magnetic structure when a magnetic field  $\mathbf{H} \perp \boldsymbol{\varepsilon}$  (293°K) is switched on can be represented in analogous fashion. This change is illustrated by the schematic diagrams presented in the upper portion of Fig. 4. (the arrows denote the spin axes of the structural blocks T). In weak fields  $H < 800-1500$  Oe the structure is quasihelical  $\omega = 120^\circ$  ( $\tau = c$ ). On increasing the field the rotation of the spin axes and the angle  $\omega$  increase to  $180^\circ$  ( $\tau = \frac{2}{3}c$ ). We explain the gradual change in the intensity of the satellites in the range of fields between 1500 and 7000 Oe by the existence in the crystal of regions with quasihelical and collinear spin ordering; this is also manifested by the increase in the magnetic contribution to the structure magnetic 009 reflection (Fig. 4).

#### 4. PROBABLE REASONS FOR THE APPEARANCE OF QUASIHHELICAL ORDERING

A comparison of the measured neutron diffraction intensities with those calculated on the basis of various

models of spin ordering compels us to accept the quasi-helical model of the spin structure for the hexagonal ferrites  $(\text{Ba}, \text{Sr})_2\text{Zn}_2\text{Fe}_{12}\text{O}_{22}$ . This structure differs considerably from the well-known types of spin configurations, including the helicoidal ordering, and also from the usual collinear structure of the unsubstituted barium ferrite  $\text{Ba}_2\text{Zn}_2\text{Fe}_{12}\text{O}_{22}$ .

In the structure of the barium ferrite  $\text{Ba}_2\text{Zn}_2\text{Fe}_{12}\text{O}_{22}$  the 6c tetrahedra ( $z = 0.0428$ ) closest to the barium ions are occupied by iron and zinc ions. On replacing the barium ions by strontium ions which have a considerably smaller ionic radius a change is possible in the shape and dimension of these polyhedra. It can be assumed that the zinc ions which "prefer" a tetrahedral coordination go over into 6c ( $z = 0.152$ ) tetrahedra, freeing their places for the iron ions. As a result the structure breaks up into blocks perpendicular to the C axis; the boundaries of these blocks are formed by layers of tetrahedra preferentially occupied by zinc ions. Within these blocks there exists a strong exchange bonding between the magnetic ions which leads to spin collinearity. The presence in the structure of intervening layers of nonmagnetic ions leads to a change in the lengths and angles of the exchange bonds of the iron ions lying in neighboring blocks, as a result of which one can expect a redistribution of the exchange-interaction energy, and as a consequence the destruction of the collinearity of the spin axes of the T blocks.

This assumption is favored by the experiment conducted within the framework of this work.

$\text{Ba}_{0.4}\text{Sr}_{1.6}\text{Co}_2\text{Fe}_{12}\text{O}_{22}$  ferrite crystals were grown which differed from those previously investigated in that all the zinc was replaced by cobalt. No magnetic superstructure was observed in the neutron diffraction patterns of these crystals. It turned out to be possible to calculate the magnetic contributions to the structure reflections on the basis of a scheme of collinear spin ordering proposed by Gorter for type-Y ferrites.

The authors express their deep gratitude to T. M. Perekalina for placing at their disposal the data of the magnetic measurements, V. V. Lider for carrying out the x-ray fluorescence analysis of the investigated samples, and R. P. Ozerov for a useful discussion of the results.

<sup>3</sup>R. O. Savage and A. Tauber, *J. Amer. Cer. Soc.* **47**, 13 (1964).

<sup>4</sup>E. W. Gorter, *Proc. IEE*, Suppl. **104B**, 252 (1957).

<sup>5</sup>P. W. Anderson, *Phys. Rev.* **79**, 705 (1950).

<sup>6</sup>H. A. Kramers, *Physika* **1**, 182 (1954).

<sup>7</sup>E. F. Bertaut, A. Deschamps, P. Pauthenet, and S. Pickart, *J. Phys. et Rad.* **20**, 404 (1950).

<sup>8</sup>J. H. Goedkoop, J. Hvoslef, and M. Zivadinovic, *Acta Cryst.* **12**, 476 (1959).

<sup>9</sup>T. Takesi, *Ferrity (Ferrites)*, Metallurg, 1964.

<sup>10</sup>L. R. Bickford, *J. Phys. Soc. Japan* **17**, Suppl. B1, 272 (1962).

<sup>11</sup>T. M. Perekalina and A. V. Zaleskii, *Zh. Eksp. Teor. Fiz.* **46**, 1985 (1964) [*Sov. Phys.-JETP* **19**, 1337 (1964)].

<sup>12</sup>I. I. Yamzin, R. A. Sizov, I. S. Zheludev, T. M. Perekalina, and A. V. Zaleskii, *Zh. Eksp. Teor. Fiz.* **50**, 595 (1966) [*Sov. Phys.-JETP* **23**, 395 (1966)].

<sup>13</sup>U. Enz, *J. Appl. Phys.*, Suppl., **32**, No. 3, 22S (1961).

<sup>14</sup>I. I. Yamzin, V. E. Staritsyn, and Yu. Z. Nozik, *Kristallografiya* **7**, 72 (1962) [*Sov. Phys.-Crystallogr.* **7**, 58 (1962)].

<sup>15</sup>I. I. Yamzin, Yu. S. Kuz'minov, V. E. Staritsyn, and E. I. Mal'tsev, *Kristallografiya* **8**, 302 (1963) [*Sov. Phys.-Crystallogr.* **8**, 234 (1963)].

<sup>16</sup>T. M. Perekalina, V. A. Sizov, R. A. Sizov, I. I. Yamsin, and R. A. Voskanyan, *Zh. Eksp. Teor. Fiz.* **52**, 409 (1967) [*Sov. Phys.-JETP* **25**, 266 (1967)].

<sup>17</sup>A. Herpin, P. Meriel, and J. Villain, *Compt. rend.* **249**, 1334 (1959).

<sup>18</sup>A. Yoshimori, *J. Phys. Soc. Japan* **14**, 807 (1969).

<sup>19</sup>W. C. Koehler, *Acta Cryst.* **14**, 535 (1961).

<sup>20</sup>D. H. Lyons, T. A. Kaplan, K. Dwight, and N. Menyuk, *Phys. Rev.* **126**, 556 (1962).

<sup>21</sup>J. M. Hastings and L. M. Corliss, *Phys. Rev.* **125**, 556 (1962).

<sup>22</sup>D. E. Cox, W. J. Takei, and G. Shirane, *J. Phys. Chem. Solids* **24**, 405 (1963).

<sup>23</sup>W. C. Koehler, J. W. Cable, M. K. Wilkinson, and E. O. Wollan, *Phys. Rev.* **151**, 414 (1966).

<sup>24</sup>R. Nathans, S. J. Pickart, and H. A. Alperin, *J. Phys. Soc. Japan* **17**, Suppl. B3, 7 (1962).

<sup>25</sup>W. C. Hamilton, *Phys. Rev.* **110**, 1050 (1958).

<sup>1</sup>P. B. Braun, *Philips Res. Rep.* **12**, 491 (1957).

<sup>2</sup>J. A. Kohn and D. W. Eckart, *Z. Kristallographie* **119**, 454 (1964).